MDPI

Article

Melt-Crystallizations of α and γ Forms of Isotactic Polypropylene in Propene-Butene Copolymers

Miriam Scoti *, **Fabio De Stefano**, **Filomena Piscitelli †**, **Giovanni Talarico**, **Angelo Giordano** and **Claudio De Rosa ***

Dipartimento di Scienze Chimiche, Università di Napoli Federico II, Complesso Monte S. Angelo, Via Cintia, 80126 Napoli, Italy

* Correspondence: miriam.scoti@unina.it (M.S.); claudio.derosa@unina.it (C.D.R.)

† Current address: Department of Materials and Structures, CIRA—Italian Aerospace Research Centre, Via Maiorise, 81043 Capua, Italy.

Abstract: Random isotactic propene-butene copolymers (iPPC4) of different stereoregularity have been synthesized with three different homogeneous single center metallocene catalysts having different stereoselectivity. All samples crystallize from the polymerization solution in mixtures of α and γ forms, and the relative amount of γ form increases with increasing concentrations of butene and of *rr* stereodefects. All samples crystallize from the melt in mixtures of α and γ forms and the fraction of γ form increases with decreasing cooling rate. At high cooling rates, the crystallization of the α form is always favored, even for samples that contain high total concentration of defects that should crystallize in the γ form. The results demonstrate that in iPPs containing significant concentrations of defects, such as stereodefects and comonomeric units, the γ form is the thermodynamically stable form of iPP and crystallizes in selective conditions of very slow crystallization, whereas the α form is the kinetically favored form and crystallizes in conditions of fast crystallization.

Keywords: propylene-butene copolymers; α and γ forms; metallocene catalysts; melt-crystallization

1. Introduction

The crystallization of α and γ forms of isotactic polypropylene (iPP) depends on the conditions of crystallization and on the molecular structure of polypropylene; the latter depends on the polymerization conditions and catalysis [1]. Different conditions of polymerization and used catalysts produce iPP macromolecules characterized by different molecular structures, because different catalysts may introduce different types and amounts of microstructural defects, such as defects of stereoregularity and regioregularity, constitutional defects and different distribution of defects along the chains [1–5].

The α form is considered the most stable form of iPP and crystallizes usually in the iPP homopoymer prepared with heterogeneous Ziegler-Natta catalysts in common crystallization conditions from the melt or from solution, and in stretched fibers [6–8]. In the same commercial iPP samples the γ form crystallizes only in special conditions, as in samples of low molecular mass [9–13] and by crystallization at high pressures [14–18]. A low amount of γ form has also been obtained in some copolymers of propylene with different comonomers synthesized with the same heterogeneous catalysts [19–47]. The γ form crystallizes, instead, easily in iPP samples [48–54] and its copolymers [55–92] synthesized with homogeneous single site metallocene catalysts [2–5], which introduce different kinds of defects depending on the catalyst structure. These defects, as stereo-defects, regio-defects and also comonomers, indeed, favors crystallization of the γ form [48–92].

The crystallization of the γ form in chains containing defects is due to the fact that the γ form crystallizes when iPP chains are characterized by short regular propene sequences, therefore, it occurs when iPP chains contain any type of defect that interrupts and shortens the regular propene sequences [51,54,62,79]. In particular, iPPs and copolymers produced

with homogeneous single site metallocene catalysts are characterized by a perfectly random distribution of defects along the macromolecules, which, therefore, shortens the length of the regular propene sequences even for low concentrations of defects [51,54,62,79].

The crystallization of α form is, instead, favored when the regular propene sequences are very long, which are generated when the concentration of defects is low or when defects are segregated in blocks of the macromolecules [51,54,62,79], as, for instance, in samples synthesized with Ziegler-Natta catalysts, where the non-random distribution of defects and their segregation in blocks make the regular propene sequences always long even in the case of a high concentration of defects and in copolymers with relatively high comonomer concentration [93–96].

Understanding the conditions of crystallization of α and γ forms of iPP is of particular relevance since the two different polymorphs exhibit significant differences in mechanical behavior [7,46,47,54,76,77,79,87–91,97–101]. In general, the molecular architecture and topology of copolymers, from standard random to block or multiblock copolymers, greatly affects the crystallization behavior and properties of polymers because of the different length of crystallizable sequences [93–96,102,103]. While the effect of the molecular structure and architecture on the crystallization behavior of iPP has been extensively investigated and the effect of different kinds of defects on the crystallization of α and γ forms has been clarified, the effect of the conditions of crystallization is still unclear.

In this paper we report a study of the crystallization of α and γ forms of iPP in propene-butene copolymers in different crystallization conditions to analyze the thermodynamic and kinetics effects on the crystallization of the two polymorphic forms. Propene-butene copolymers of different stereoregularity synthesized with different metallocene catalysts have been chosen for this study because they crystallize easily in the γ form, thanks to the incorporation in the iPP chains of butene comonomeric units that shorten the length of the regular propene sequences [79]. Hence, in this system, the γ form is the thermodynamically stable form of iPP and, therefore, these copolymers represent the ideal system to study the crystallization conditions that may favor crystallization of the α form.

2. Materials and Methods

Propylene-butene isotactic copolymers (iPPC4) were synthesized with the metallocene catalysts of Scheme 1 having different stereoselectivity activated with methylalumoxane (MAO) (from Lanxess, Cologne, Germany) [79]. All operations were performed under nitrogen by using conventional Schlenk-line techniques. Toluene solvent was purified by degassing with N_2 and passing over activated Al_2O_3 (8 h, N_2 purge, 300 °C), and stored under nitrogen. The MAO cocatalyst was used as received (10 wt.%/vol. toluene solution, 1.7 M in Al). The catalyst mixture was prepared by dissolving the desired amount of the metallocene with the proper amount of the MAO solution, obtaining a solution which was stirred for 10 min at 25 °C before being injected into the reactor. All copolymerizations were run at 25 °C in a 250 mL Pyrex reactor, agitated with magnetic stirrer, containing toluene (100 mL) and MAO (2.0 mL). Gas mixtures of propene and 1-butene at the appropriate composition, prepared with vacuum line techniques in a gas cylinder at pressure of 4–5 bar and standardized by gas chromatography, were bubbled through the liquid phase at atmospheric pressure and a flow rate of 0.3 L/min. The polymerizations started by syringing in the toluene solution of the catalyst (2–3 mg) and proceeded under a constant flow of the gas mixture. Under such conditions, total monomer conversions were lower than 15%, this ensuring a nearly constant feeding ratio. The copolymers were coagulated with excess methanol acidified with enough HCl (aqueous, concentrated) to prevent the precipitation of alumina from MAO hydrolysis, filtered, washed with further methanol, and vacuum-dried. Typical yields were 2–5 g with a 120 min reaction time.
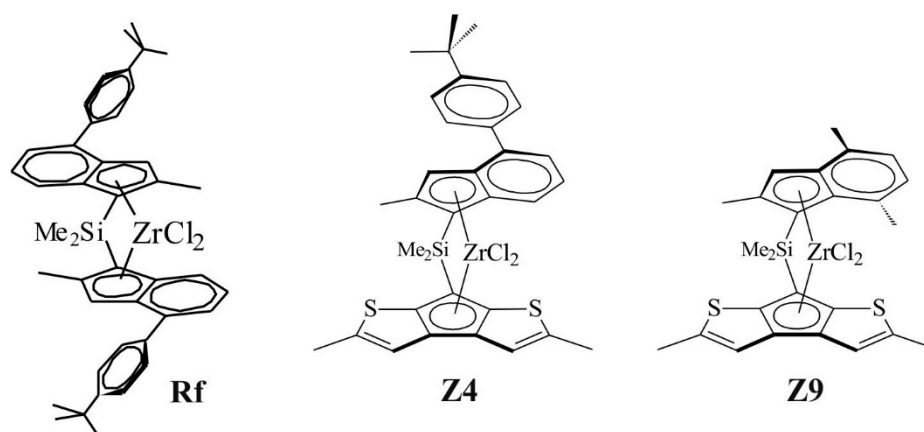
Scheme 1. Structures of the isoselective C2-symmetric (Rf) and less isoselective C1-symmetric (Z4 and Z9) metallocene catalysts used for the synthesis of iPPC4 copolymers.

The C_2-symmetric metallocene Rf is highly isospecific [104,105] and produces highly isotactic iPPC4 copolymers (samples iPPC4Rf-x, where x is the butene concentration) containing negligible amounts of stereodefects (lower than 0.1 mol% of *rr* triads) and small amount of regiodefects around 0.1–0.5 mol%, represented by secondary 2,1-erythro units (2,1e). The two C_1-symmetric metallocenes Z4 and Z9 are instead fully regioselective but introduce significant amounts of *rr* stereodefects [106–109]. Samples of iPPC4 copolymers synthesized with the catalyst Z4 (sample iPPC4Z4-x) are fully regioregular and contain 2.0–2.4 mol% of *rr* stereodefects, whereas samples synthesized with the catalyst Z9 (samples iPPC4Z9-x) contain 2.5–3.4 mol% of *rr* defects [107,108]. Consequently, the less isotactic samples synthesized with catalysts Z4 and Z9 show melting temperatures lower than those of the samples synthesized with the catalyst Rf [79]. The composition, the melting temperatures and the molecular mass of all samples are shown in Table 1.

Table 1. Catalyst, composition (mol% butene), melting temperature of as-prepared samples (T_m), molecular mass (M_w) and dispersity (M_w/M_n) of the iPPC4 copolymers [79].

Sample	Catalyst	mol% Butene	T_m (°C) [a]	M_w [b]	M_w/M_n [b]
iPPC4Rf-1	Rf	1.9	143	316,500	2.2
iPPC4Rf-2	Rf	4.3	137	228,700	2.1
iPPC4Rf-3	Rf	4.5	137	207,000	2.0
iPPC4Rf-4	Rf	8.0	125	178,500	2.0
iPPC4Rf-5	Rf	9.0	120	200,000	2.1
iPPC4Z4-1	Z4	1.3	135	172,900	2.1
iPPC4Z4-2	Z4	4.6	123	175,700	2.0
iPPC4Z4-3	Z4	8.2	112	176,700	2.0
iPPC4Z9-1	Z9	1.4	126	214,000	2.1
iPPC4Z9-2	Z9	2.2	124	214,500	2.0
iPPC4Z9-3	Z9	6.4	113	214,400	2.0

[a] Determined from DSC heating curves recorded at 10 °C/min. [b] Determined by GPC.

The composition and comonomer distribution were determined by ^{13}C NMR analysis (Table 1). All spectra were obtained using a Bruker DPX-400 spectrometer operating in the Fourier transform mode at 120 °C at 100.61 MHz (Bruker Company, Billerica, MA, USA). The samples were dissolved with 8% wt/v concentration in 1,1,2,2-tetrachloroethane-d_2 at 120 °C. The carbon spectra were acquired with a 90° pulse and 15 s of delay between pulses and CPD (WALTZ 16) to remove ^1H-^{13}C coupling. About 1500–3000 transients were stored in 32K data points using a spectral window of 6000 Hz. For all copolymer samples, the peak of the propylene methine carbon atoms was used as internal reference at 28.83 ppm. The ^{13}C NMR spectra of two samples of iPPC4 copolymers are reported in Figure S1 of

the Supplementary Material. The resonances were assigned according to ref. [110] and the butene concentrations in the copolymers were evaluated from the concentrations of the constitutional diads PP, PB, BB (P = propene, B = butene), using the Equations S1–S5 of the Supplementary Material. The NMR analysis showed that all the copolymers present a random distribution of comonomers and homogeneous intermolecular composition with $r_P \times r_B \approx 1$, calculated using the Equation S6 of the Supplementary Material, according to ref. [111].

The molecular masses and the dispersity were determined by gel permeation chromatography (GPC), using a Polymer Laboratories GPC220 apparatus equipped with a differential refractive index (RI) detector and a Viscotek 220R viscometer (Agilent Company, Santa Clara, CA, USA), on polymer solutions in 1,2,4-trichlorobenzene at 135 °C of 2 mg/mL concentration. The injection volume was 300 µL with a flow rate of 1.0 mL/min. The GPC apparatus was calibrated with 12 standard samples of polystyrene having narrow dispersity and molecular masses in the range 580 and 13.2×10^6.

The calorimetry measurements were carried out with differential scanning calorimeter (DSC) Mettler Toledo DSC-822 (Columbus, OH, USA) performing scans in a flowing N_2 atmosphere and scanning rate of 10 °C/min.
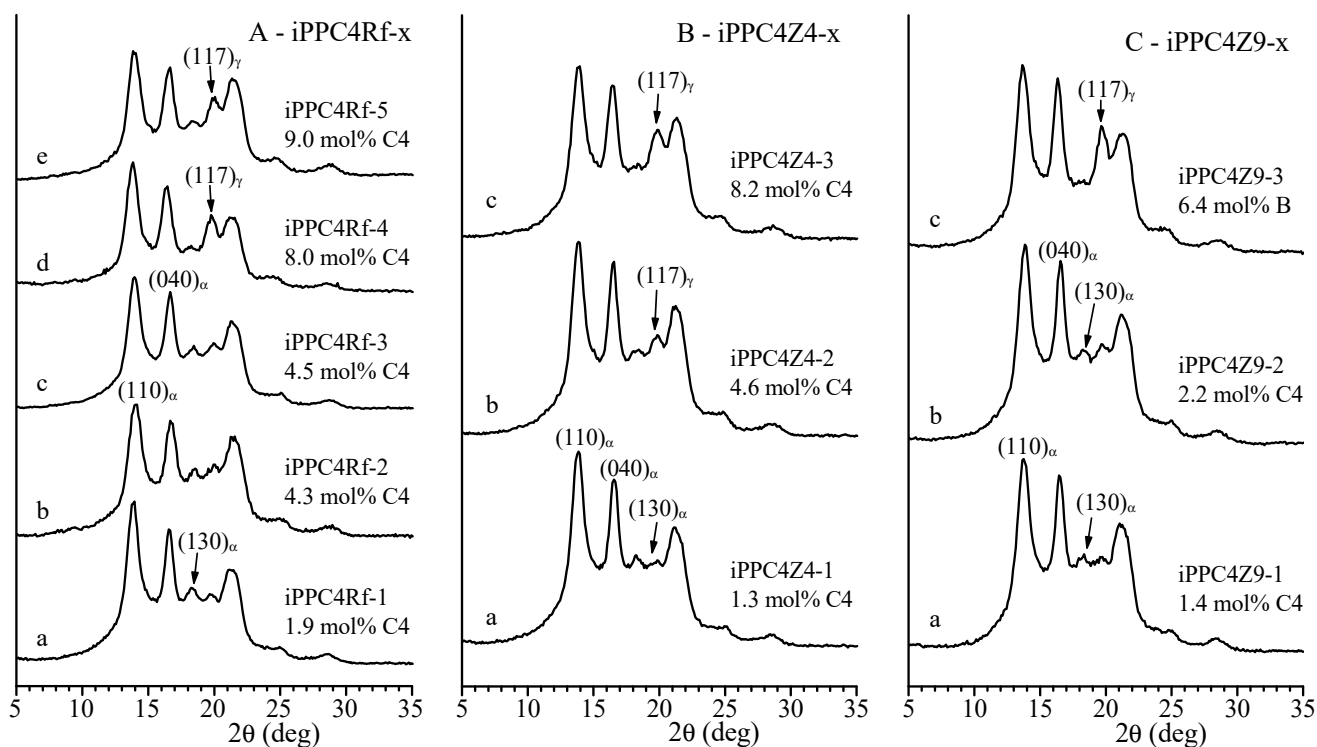
X-ray powder diffraction profiles were recorded with Ni filtered Cu Kα radiation by using an Empyrean diffractometer (Malvern Panalytical, Worcestershire, UK).

All samples of iPPC4 copolymers were crystallized in DSC by cooling the melt at 180 °C down to 25 °C at different cooling rates from 1 to 40 °C/min. After the crystallization in DSC, the samples were analyzed by X-ray diffraction.

In samples that crystallized in mixtures of α and γ forms, the relative fraction of the γ form f_γ, with respect to the α form, was calculated from the intensities of the $(117)_\gamma$ and $(130)_\alpha$ reflections at 2θ = 20.1° of the γ form and at 2θ = 18.6° of the α form, respectively, as the ratio: $f_\gamma = I(117)_\gamma / [I(117)_\gamma + I(130)_\alpha]$.

3. Results and Discussion

The X-ray diffraction profiles of as-prepared (precipitated from the polymerization solution) samples of iPPC4 copolymers of Table 1 are reported in Figure 1. The diffraction profiles present the $(130)_\alpha$ and $(117)_\gamma$ reflections at 2θ = 18.6 and 20.1° of the α and γ forms, respectively, indicating that all as-prepared samples of iPPC4 copolymers are crystallized in mixtures of α and γ forms. The intensity of the $(117)_\gamma$ reflection increases with increasing butene concentration and, at the same butene content, is higher in the low stereoregular samples synthesized with the catalysts Z4 and Z9 (samples iPPC4Z4-x and iPPC4Z9-x, Figure 1B,C). The values of the relative amount of γ form (f_γ) calculated from the intensities of the $(117)_\gamma$ and $(130)_\alpha$ reflections in the diffraction profiles of Figure 1 are reported in Figure 2 as a function of butene concentration. Since the highly stereoregular iPP homopolymer generally crystallizes in the α form, it has been assumed $f_\gamma = 0$ for butene concentration equal to zero. It is apparent that the amount of γ form increases with increasing concentration of butene and of *rr* stereodefects [79] (Figure 2). The more isotactic samples iPPC4Rf-x crystallize almost in the pure γ form ($f_\gamma \approx 80\%$) for butene concentration of nearly 9 mol% (sample iPPC4Rf-5, profile e in Figures 1A and 2), whereas for the less isotactic samples iPPC4Z9-x, the highest amount of γ form ($f_\gamma \approx 88\%$) crystallizes at about 6 mol% of butene (sample iPPC4Z9-3, profile c in Figures 1C and 2).
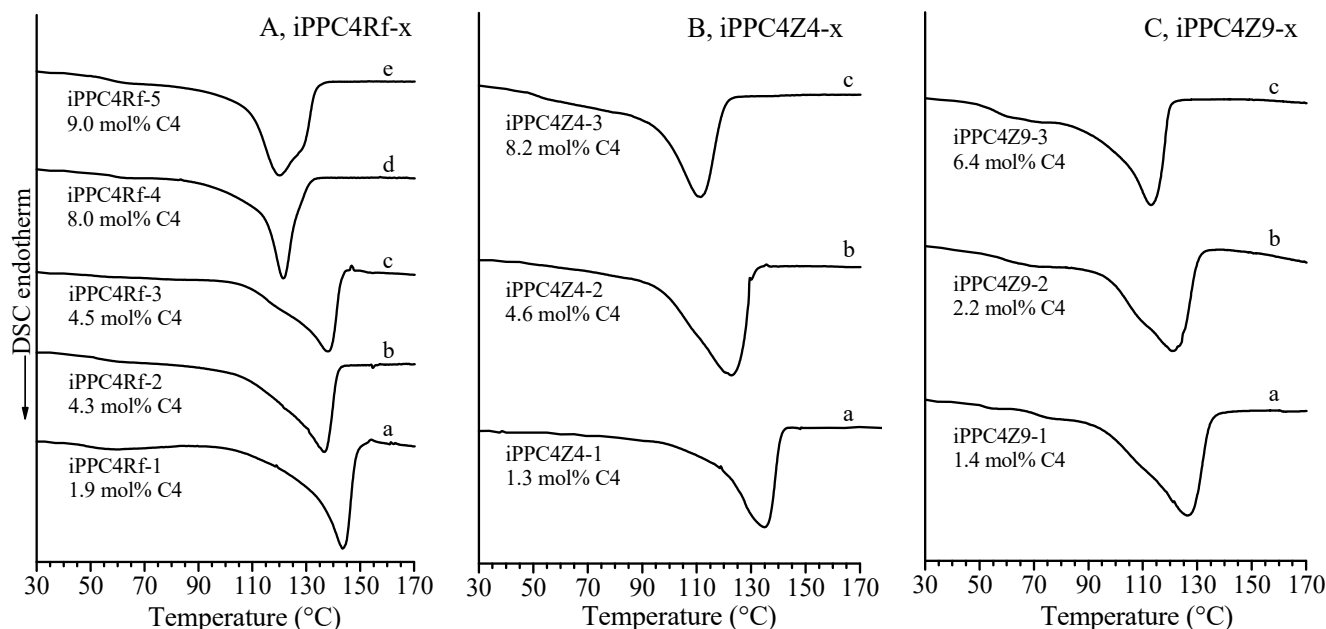
Figure 1. X-ray powder diffraction profiles of as-prepared samples of iPPC4 copolymers of the indicated butene concentration. Isotactic samples iPPC4Rf-x with $[rr] < 0.1$ mol% (**A**) and less isotactic samples iPPC4Z4-x with $[rr] = 2.0–2.4$ mol% (**B**) and iPPC4Z9-x with $[rr] = 2.5–3.4$ mol% (**C**).
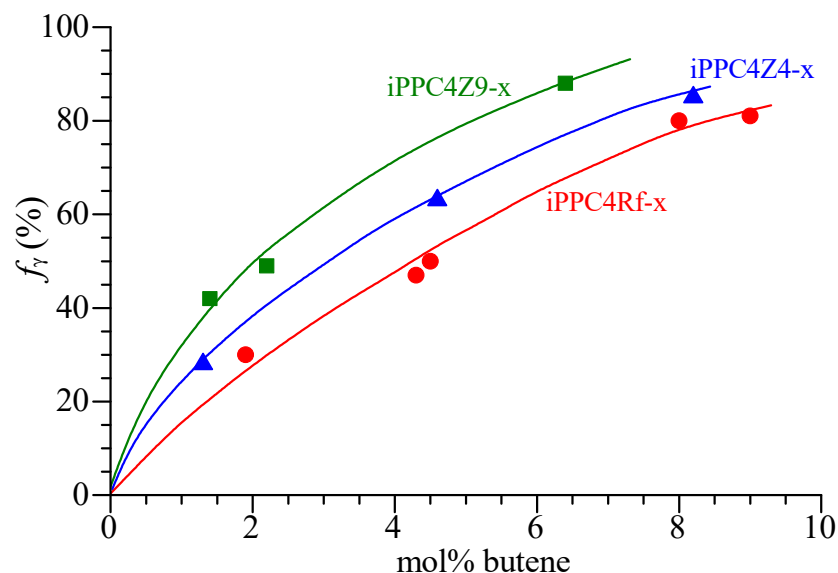
Figure 2. Values of the fraction of γ form that crystallizes in the as-prepared samples of iPPC4 copolymers as a function of butene concentration evaluated from the diffraction profiles of Figure 1. Isotactic samples iPPC4Rf-x with $[rr] < 0.1$ mol% (●) and less isotactic samples iPPC4Z4-x with $[rr] = 2.0–2.4$ mol% (▲) and iPPC4Z9-x with $[rr] = 2.5–3.4$ mol% (■).

It is worth reminding that in iPPC4 copolymers the further increase of butene concentration induces decrease of the amount of γ form and crystallization of the α form for concentrations higher than 15–20 mol% because butene units are included easily in the crystals of α form producing stabilization of the α form compared to the γ form [79].

The DSC heating curves of the as-polymerized samples of iPPC4 copolymers are reported in Figure 3. For the three sets of samples the melting temperature decreases with increasing butene concentration. The values of the melting temperature are reported in Table 1 and in Figure 4A as a function of butene concentration.


Figure 3. DSC heating curves recorded at 10 °C/min of as-prepared samples of iPPC4 copolymers of the indicated butene concentration. Isotactic samples iPPC4Rf-x with [*rr*] < 0.1 mol% (**A**) and less isotactic samples iPPC4Z4-x with [*rr*] = 2.0–2.4 mol% (**B**) and iPPC4Z9-x with [*rr*] = 2.5–3.4 mol% (**C**).

It is apparent from Figure 4A that the melting temperature also depends on the stereoregularity of the samples and on the concentration of *rr* defects. In fact, at the same butene concentration the more isotactic samples iPPC4Rf-x show melting temperatures higher than those of the less isotactic samples iPPC4Z4-x and iPPC4Z9-x, and the samples iPPC4Z9-x with the highest concentration of *rr* stereodefects show the lowest melting temperatures.

All samples have been crystallized in DSC from the melt by cooling at different cooling rates. The samples have been melted by heating at 10 °C/min up to 170 °C, as in Figure 3, and then cooled from 170 °C down to 25 °C at different cooling rates, from 1 °C/min to 40 °C/min. As an example, the DSC cooling curves of all samples recorded at cooling rate of 10 °C/min are reported in Figure 5. All samples crystallize during cooling and the DSC curves of Figure 5 show well-defined exothermic peaks. The values of the crystallization temperature evaluated from the DSC cooling curves of Figure 5 at cooling rate of 10 °C/min are plotted in Figure 4B as a function of butene concentration. For the three sets of samples, the crystallization temperature decreases with increasing butene concentration and, at the same butene concentration, decreasing the stereoregularity (Figure 4B). Therefore, introduction of both butene co-units and *rr* stereodefects produces a decrease of melting and crystallization temperatures (Figure 4) and an increase of the fraction of γ form (Figure 2).

After the crystallization in DSC as in Figure 5, the samples were analyzed by X-ray diffraction at 25 °C. The diffraction profiles of the samples iPPC4Rf-x, iPPC4Z4-x and iPPC4Z9-x crystallized from the melt at different cooling rates are reported in Figures 6–8, respectively. All samples crystallize into mixtures of α and γ forms and the amounts of the two forms strongly depend on the cooling rate.
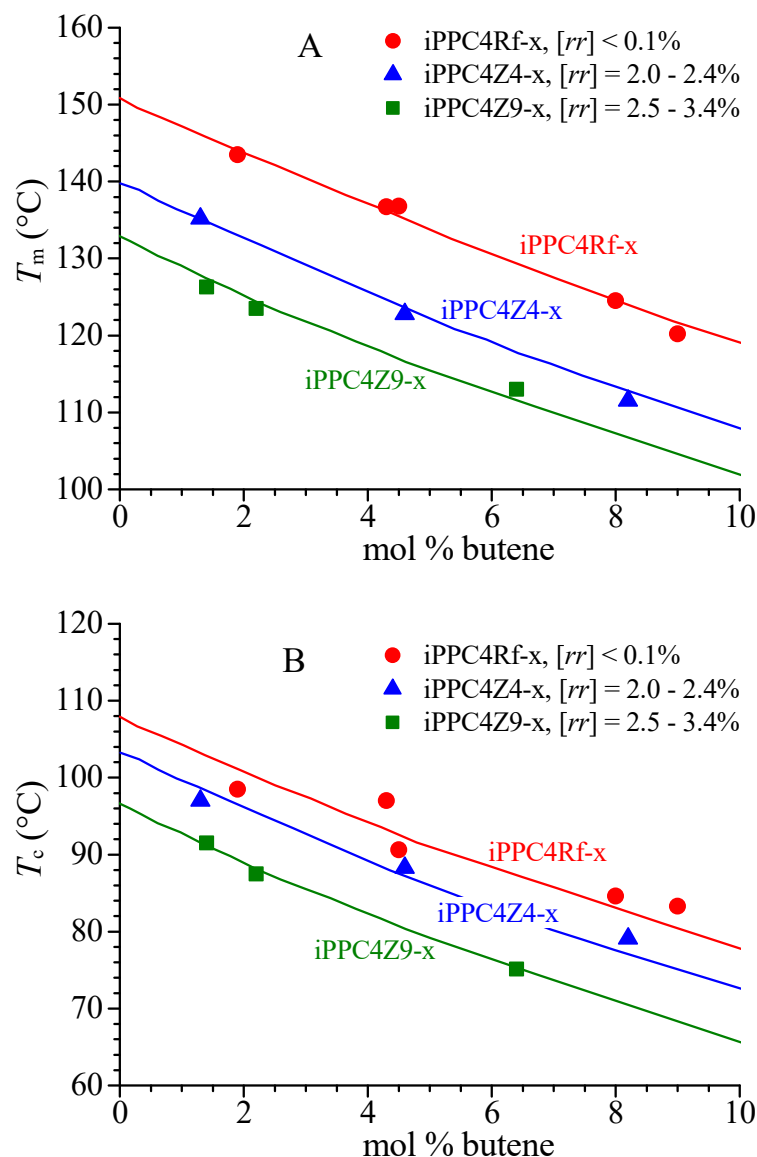
Figure 4. Melting temperature of the as-prepared samples (**A**) and crystallization temperature from the melt (**B**) of iPPC4 copolymers as a function of butene concentration evaluated from DSC thermograms recorded at scanning rates of 10 °C/min. Isotactic samples iPPC4Rf-x with [*rr*] < 0.1 mol% (•) and less isotactic samples iPPC4Z4-x with [*rr*] = 2.0–2.4 mol% (▲) and iPPC4Z9-x with [*rr*] = 2.5–3.4 mol% (■).

The samples displayed the same behavior regardless of the butene concentration and stereoregularity, that is, the intensity of the $(130)_\alpha$ reflection of the α form at $2\theta = 18.6°$ decreases and the intensity of the $(117)_\gamma$ reflection at $2\theta = 20.1°$ of the γ form increases with decreasing cooling rate. The amount of γ form is reported in Figure 9 as a function of the cooling rate for the three sets of samples. These data indicate that the amount of γ form increases with decreasing cooling rate. Correspondingly, the γ form almost disappears and the almost pure α form crystallizes in all samples at the highest cooling rate of 40 °C/min (profiles e of Figures 6–8). The highest concentration of γ form is always obtained at low cooling rates, whereas at high cooling rates the crystallization of the α form is always favored, even for samples that contain high total concentration of defects (high butene and high *rr* defects concentrations) that tend to crystallize normally in the γ form. In fact, even the less isotactic samples iPPC4Z4-3 and iPPC4Z9-3 with the highest butene concentrations of 8.2 and 6.4 mol%, respectively, that crystallize in the as-prepared samples in the almost

pure γ form (f_γ = 85 and 88%, respectively) (profiles c of Figures 1B,C and 2), crystallize in the α form in the fast crystallization from the melt at high cooling rate (profiles e of Figures 7 and 8).
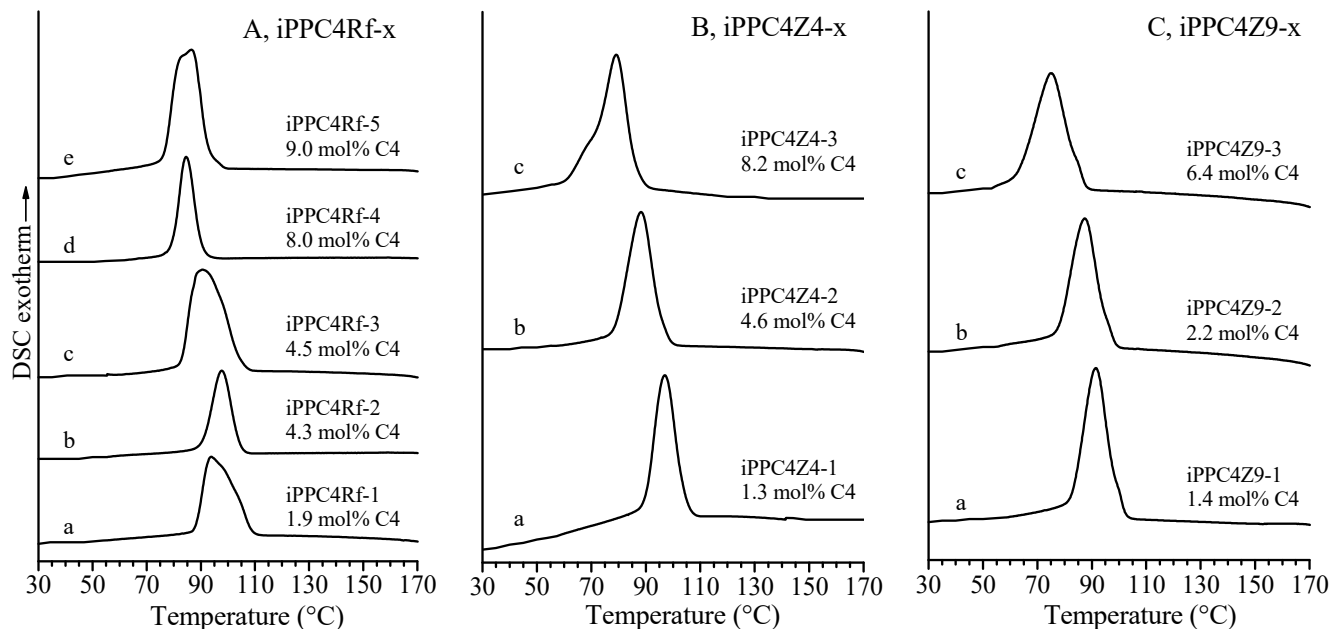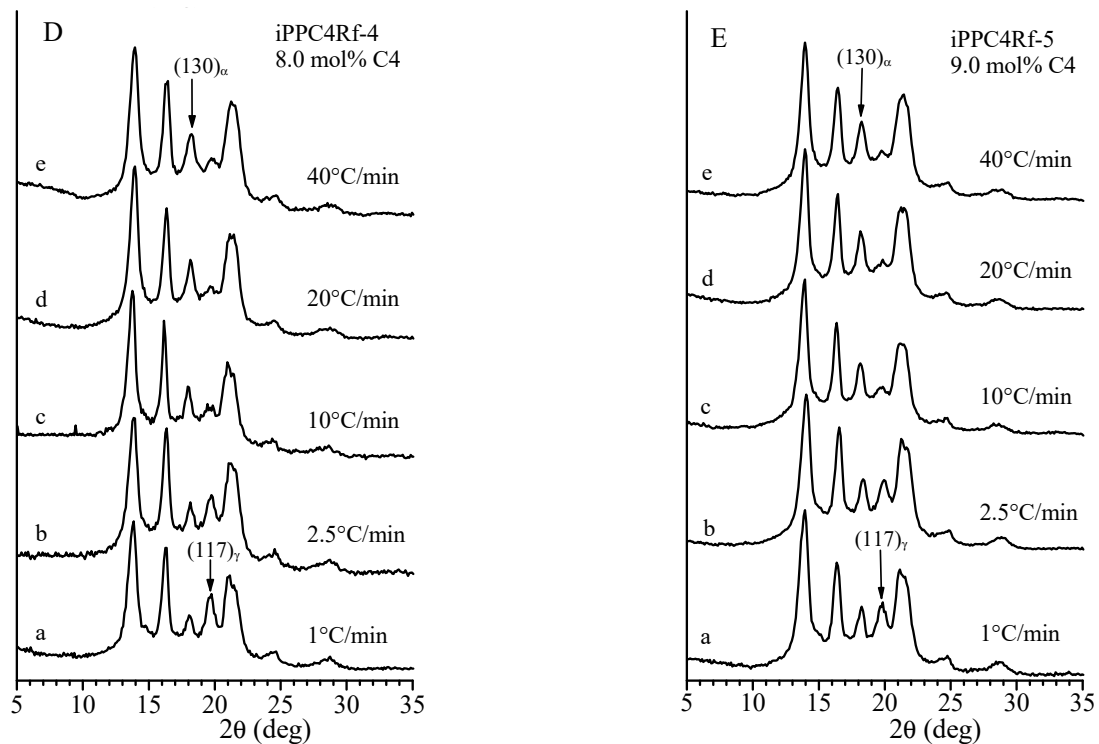

Figure 5. DSC cooling curves recorded at 10 °C/min of samples of iPPC4 copolymers of the indicated butene concentration after melting at 170 °C (Figure 3). Isotactic samples iPPC4Rf-x with [*rr*] < 0.1 mol% (**A**) and less isotactic samples iPPC4Z4-x with [*rr*] = 2.0–2.4 mol% (**B**) and iPPC4Z9-x with [*rr*] = 2.5–3.4 mol% (**C**).
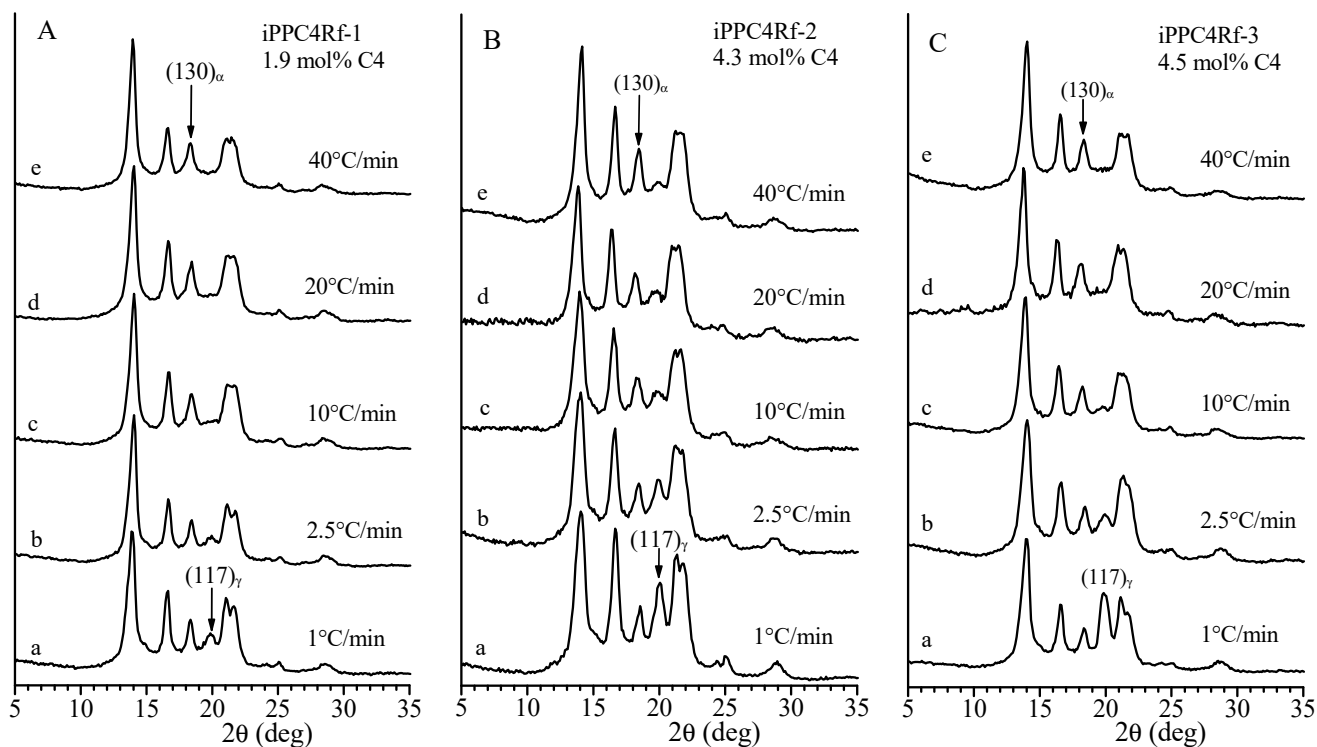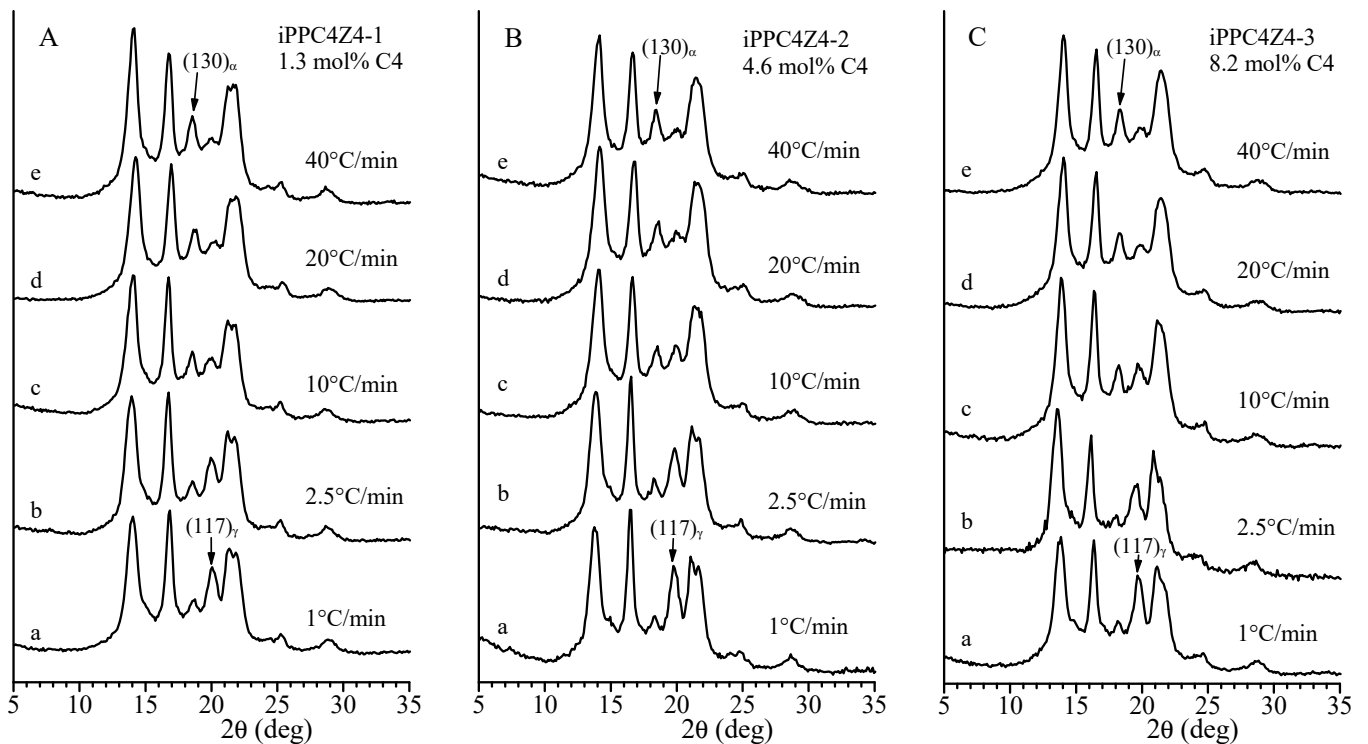

Figure 6. *Cont.*

Figure 6. X-ray diffraction profiles of samples of copolymers iPPC4Rf-x crystallized from the melt by cooling the melt from 170 °C down to 25 °C at the indicated different cooling rates.

Figure 7. X-ray diffraction profiles of samples of copolymers iPPC4Z4-x crystallized from the melt by cooling the melt from 170 °C down to 25 °C at the indicated different cooling rates.
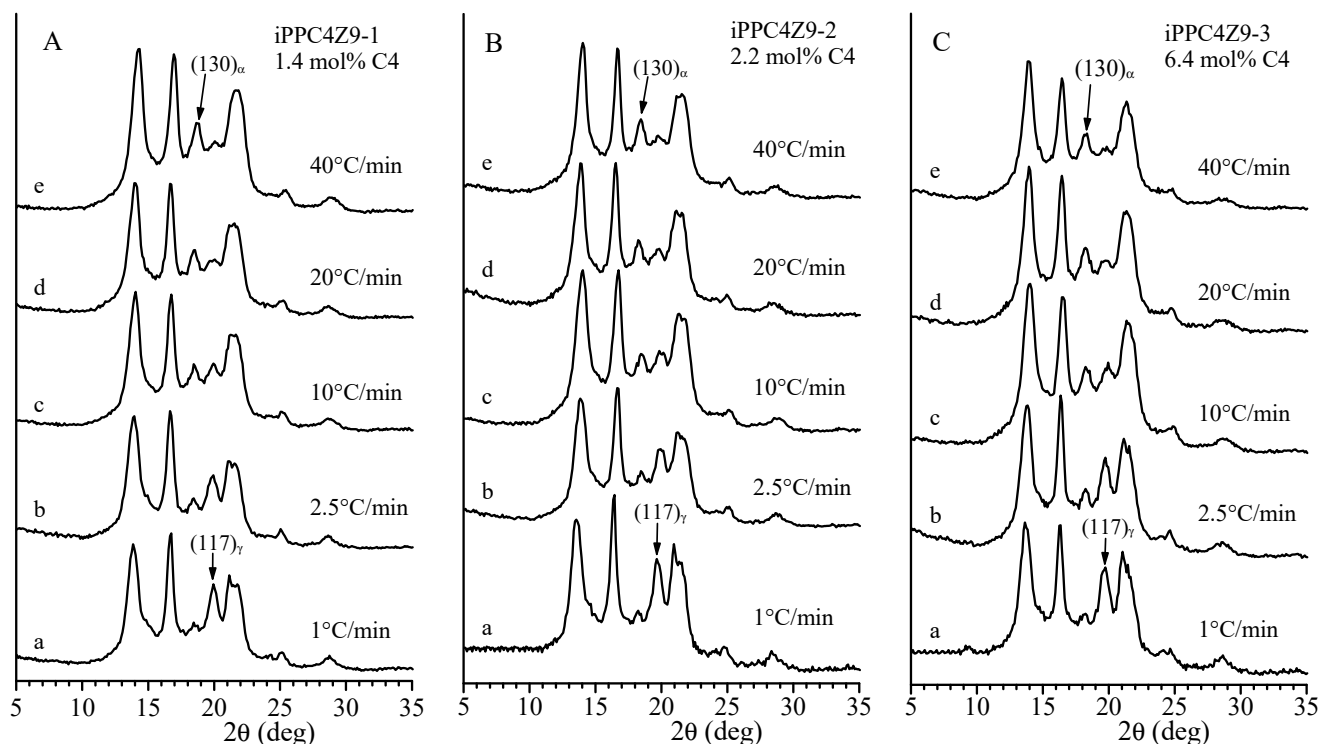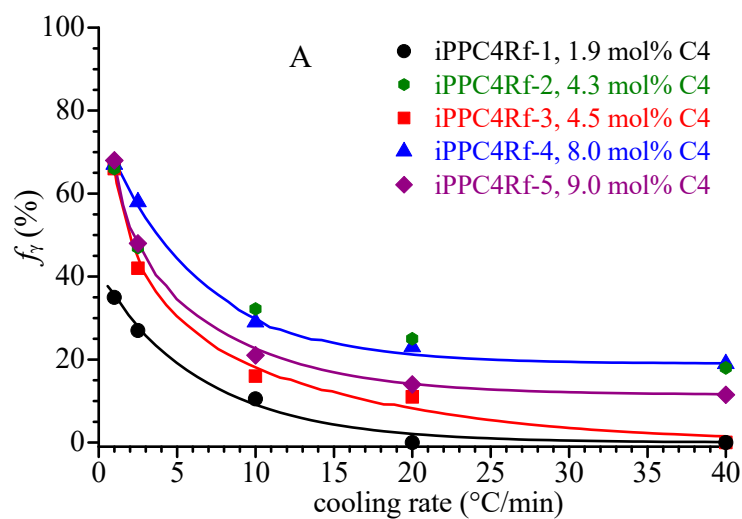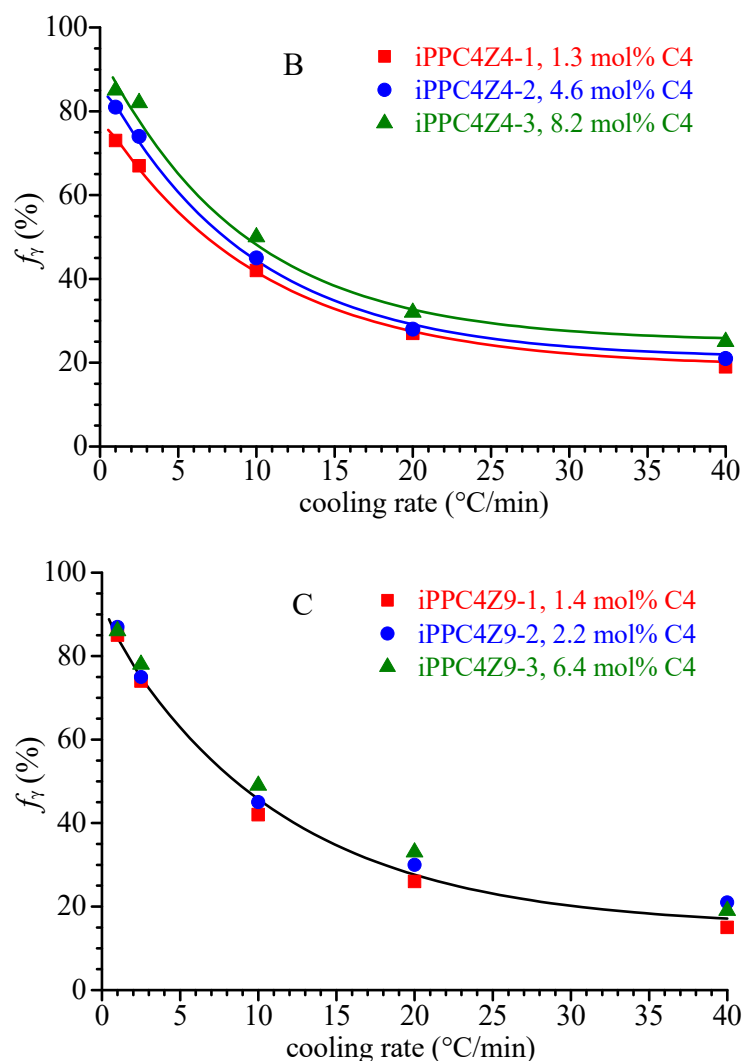
Figure 8. X-ray diffraction profiles of samples of copolymers iPPC4Z9-x crystallized from the melt by cooling the melt from 170 °C down to 25 °C at the indicated different cooling rates.

These results demonstrate that in iPP samples containing significant concentrations of defects, such as stereodefects and butene comonomeric units, the γ form is the thermodynamically stable form of iPP and crystallizes normally from polymer solution or in selective conditions of very slow crystallization, as isothermal crystallizations from the melt at high crystallization temperatures [79] or by cooling from the melt at very low cooling rates, whereas the α form is the kinetically favored form and crystallizes in conditions of fast crystallization, such as fast cooling from the melt.

Figure 9. *Cont.*

Figure 9. Values of the fraction of γ form that crystallizes in samples of iPPC4 copolymers cooled from the melt at different cooling rates as a function of the cooling rate, evaluated from the diffraction profiles of Figures 6–8. (**A**) Isotactic samples iPPC4Rf-x with [*rr*] < 0.1 mol%, (**B**) samples iPPC4Z4-x with [*rr*] = 2.0–2.4 mol%, and (**C**) samples iPPC4Z9-x with [*rr*] = 2.5–3.4 mol%.

4. Conclusions

Random isotactic propene-butene copolymers of different stereoregularity have been prepared with three different metallocene catalysts having different stereoselectivity. The C_2-symmetric metallocene produces highly isotactic iPPC4 copolymers containing negligible amounts of stereodefects, whereas the two C_1-symmetric metallocenes produce less isotactic copolymers containing on average 2.0–2.4 mol% and 2.5–3.4 mol% of *rr* stereodefects, respectively.

All as-prepared samples crystallize in mixtures of α and γ forms from the polymerization solution and the relative amount of γ form increases with increasing concentrations of butene and of *rr* stereodefects.

The samples have been crystallized from the melt by cooling the melt from 170 °C down to 25 °C at different cooling rates. All samples crystallize from the melt in mixtures of α and γ forms and the amount of the two forms strongly depends on the cooling rate. The amount of γ form increases with decreasing cooling rate. Correspondingly, the γ form almost disappears and the almost pure α form crystallizes in all samples at the highest cooling rate of 40 °C/min. The highest concentration of γ form is always obtained at low cooling rates, whereas at high cooling rates the crystallization of the α form is always

favored, even for samples that contain high total concentration of defects that should crystallize in the γ form.

These results demonstrate that in iPP samples containing significant concentrations of defects, such as stereodefects and butene comonomeric units, the γ form is the thermodynamically stable form of iPP and crystallizes normally from polymer solution or in selective conditions of very slow crystallization, such as by cooling from the melt at very low cooling rates, whereas the α form is the kinetically favored form and crystallizes in conditions of fast crystallization, such as fast cooling from the melt.

References

1. Pasquini, N. (Ed.) *Polypropylene Handbook*; Hanser Publishers: Munich, Germany, 2005.
2. Ewen, J.A. Mechanisms of stereochemical control in propylene polymerizations with soluble Group 4B metallocene/methylalumoxane catalysts. *J. Am. Chem. Soc.* **1984**, *106*, 6355. [CrossRef]
3. Kaminsky, W.; Kulper, K.; Brintzinger, H.H.; Wild, F.R.W. Polymerization of propene and butene with a chiral zirconocene and methylaluminoxane as cocatalyst. *Angew. Chem.* **1985**, *97*, 507. [CrossRef]
4. Brintzinger, H.H.; Fischer, D.; Mulhaupt, R.; Rieger, B.; Waymouth, R.M. Stereospecific Olefin Polymerization with Chiral Metallocene Catalysts. *Angew. Chem. Int. Ed. Engl.* **1995**, *34*, 1143. [CrossRef]
5. Resconi, L.; Cavallo, L.; Fait, A.; Piemontesi, F. Selectivity in Propene Polymerization with Metallocene Catalysts. *Chem. Rev.* **2000**, *100*, 1253. [CrossRef]
6. Brückner, S.; Meille, S.V.; Petraccone, V.; Pirozzi, B. Polymorphism in Isotactic Polypropylene. *Prog. Polym. Sci.* **1991**, *16*, 361–404. [CrossRef]
7. De Rosa, C.; Scoti, M.; Di Girolamo, R.; Ruiz de Ballesteros, O.; Auriemma, F.; Malafronte, A. Polymorphism in polymers: A tool to tailor material's properties. *Polym. Cryst.* **2020**, *3*, e10101. [CrossRef]
8. Natta, G.; Corradini, P. Structure and properties of isotactic polypropylene. *Nuovo Cim. Suppl.* **1960**, *15*, 40. [CrossRef]
9. Lotz, B.; Graff, S.; Wittmann, J.C. Crystal morphology of the γ (triclinic) phase of isotactic polypropylene and its relation to the α phase. *J. Polym. Sci. Polym. Phys. Ed.* **1986**, *24*, 2017. [CrossRef]
10. Kojima, M. Solution-γ grown lamellar crystals of thermally decomposed isotactic polypropylene. *J. Polym. Sci. Part B: Polymer Letters* **1967**, *5*, 245. [CrossRef]
11. Kojima, M. Morphology of polypropylene crystals. III. Lamellar crystals of thermally decomposed polypropylene. *J. Polym. Sci. Part B Polym. Phys.* **1968**, *6*, 1255. [CrossRef]
12. Morrow, D.R.; Newman, B.A. Crystallization of low-molecular-weight polypropylene fractions. *J. Appl. Phys.* **1968**, *39*, 4944. [CrossRef]
13. Natta, G.; Mazzanti, G.; Crespi, G.; Moraglio, G. Polimeri isotattici e polimeri a stereoblocchi del propilene. *Chim. Ind. Milan* **1957**, *39*, 275.

14. Kardos, J.L.; Christiansen, A.W.; Baer, E. Structure of pressure crystallized polypropylene. *J. Polym. Sci. Part B Polym. Phys.* **1966**, *4*, 777. [CrossRef]

15. Pal, K.D.; Morrow, D.R.; Sauer, J.A. Interior morphology of bulk polypropylene. *Nature* **1966**, *211*, 514.

16. Mezghani, K.; Phillips, P.J. The γ-phase of high molecular weight isotactic polypropylene: III. The equilibrium melting point and the phase diagram. *Polymer* **1998**, *39*, 3735.

17. Mezghani, K.; Phillips, P.J. The γ-phase of high molecular weight isotactic polypropylene. II. The morphology of the γ-form crystallized at 200 MPa. *Polymer* **1997**, *38*, 5725.

18. Brückner, S.; Phillips, P.J.; Mezghani, K.; Meille, S.V. On the crystallization of γ-isotactic polypropylene. A high pressure study. *Macromol. Rapid Commun.* **1997**, *18*, 1. [CrossRef]

19. Turner-Jones, A. Development of the γ-crystal form in random copolymers of propylene and their analysis by DSC and X-ray methods. *Polymer* **1971**, *12*, 487–508. [CrossRef]

20. Cimmino, S.; Martuscelli, E.; Nicolais, L.; Silvestre, C. Thermal and mechanical properties of isotactic random propylene-butene-1 copolymers. *Polymer* **1978**, *19*, 1222. [CrossRef]

21. Crispino, L.; Martuscelli, E.; Pracella, M. Influence of composition on the melt crystallization of isotactic random propylene/1-butene copolymers. *Makromol. Chem.* **1980**, *181*, 1747. [CrossRef]

22. Cavallo, P.; Martuscelli, E.; Pracella, M. Effect of thermal treatment on solution grown crystals of isotactic propylene/butene-1 copolymers. *Polymer* **1997**, *18*, 891. [CrossRef]

23. Starkweather, H.W., Jr.; Van-Catledge, F.A.; MacDonald, R.N. Crystalline order in copolymers of ethylene and propylene. *Macromolecules* **1982**, *15*, 1600–1604. [CrossRef]

24. Guidetti, G.P.; Busi, P.; Giulianetti, I.; Zanetti, R. Structure-properties relationships in some random copolymers of propylene. *Eur. Polym. J.* **1983**, *19*, 757–759. [CrossRef]

25. Avella, M.; Martuscelli, E.; Della Volpe, G.; Segre, A.; Rossi, E.; Simonazzi, T. Composition-properties relationships in propene-ethene random copolymers obtained with high-yield Ziegler-Natta supported catalysts. *Makromol. Chem.* **1986**, *187*, 1927. [CrossRef]

26. Marigo, A.; Marega, C.; Zanetti, R.; Paganetto, G.; Canossa, E.; Coletta, F.; Gottardi, F. Crystallization of the γ-form of isotactic poly(propylene). *Makromol. Chem.* **1989**, *190*, 2805. [CrossRef]

27. Monasse, B.; Haudin, J.M. Effect of random copolymerization on growth transition and morphology change in polypropylene. *Colloid Polym. Sci.* **1988**, *266*, 679–687. [CrossRef]

28. Xu, Z.K.; Feng, L.X.; Wang, D.; Yang, S.L. Copolymerization of propene with 1-alkenes using a MgCl$_2$/TiCl$_4$ catalyst. *Makromol. Chem.* **1991**, *192*, 1835–1840. [CrossRef]

29. Yang, S.L.; Xu, Z.K.; Feng, L.X. Copolymerization of propene with high-1-olefin using a MgCl$_2$/TiCl$_4$ catalyst. *Makromol. Chem. Macromol. Symp.* **1992**, *63*, 233. [CrossRef]

30. Zimmermann, H.J. Structural analysis of random propylene-ethylene copolymers. *J. Macromol. Sci. Phys.* **1993**, *32*, 141–161. [CrossRef]

31. Sugano, T.; Gotoh, Y.; Fujita, T. Effect of catalyst isospecificity on the copolymerization of propene with 1-hexene. *Makromol. Chem.* **1992**, *193*, 43. [CrossRef]

32. Hingmann, R.; Rieger, J.; Kersting, M. Rheological Properties of a Partially Molten Polypropylene Random Copolymer during Annealing. *Macromolecules* **1995**, *28*, 3801. [CrossRef]

33. Morini, G.; Albizzati, E.; Balbontin, G.; Mingozzi, I.; Sacchi, M.C.; Forlini, F.; Tritto, I. Microstructure Distribution of Polypropylenes Obtained in the Presence of Traditional Phthalate/Silane and Novel Diether Donors: A Tool for Understanding the Role of Electron Donors in MgCl$_2$-Supported Ziegler−Natta Catalysts. *Macromolecules* **1996**, *29*, 5770. [CrossRef]

34. Pérez, E.; Benavente, R.; Bello, A.; Pereña, J.M.; Zucchi, D.; Sacchi, M.C. Crystallization behaviour of fractions of a copolymer of propene and 1-hexene. *Polymer* **1997**, *38*, 5411. [CrossRef]

35. Laihonen, S.; Gedde, U.W.; Werner, P.-E.; Martinez-Salazar, J. Crystallization kinetics and morphology of poly(propylene-*stat*-ethylene) fractions. *Polymer* **1997**, *38*, 361–369. [CrossRef]

36. Laihomen, S.; Gedde, U.W.; Werner, P.E.; Westdahl, M.; Jääskeläinen, P.; Martinez-Salazar, J. Crystal structure and morphology of melt-crystallized poly(propylene-*stat*-ethylene) fractions. *Polymer* **1997**, *38*, 371–377. [CrossRef]

37. Abiru, T.; Mizuno, A.; Weigand, F. Microstructural characterization of propylene–butene-1 copolymer using temperature rising elution fractionation. *J. Appl. Polym. Sci.* **1998**, *68*, 1493–1501. [CrossRef]

38. Feng, Y.; Jin, X.; Hay, J.N. Crystalline structure of propylene–ethylene copolymer fractions. *J. Appl. Polym. Sci.* **1998**, *68*, 381. [CrossRef]

39. Feng, Y.; Hay, J.N. The characterization of random propylene–ethylene copolymer. *Polymer* **1998**, *39*, 6589–6596. [CrossRef]

40. Xu, J.; Feng, Y. Application of temperature rising elution fractionation in polyolefins. *Eur. Polym. J.* **2000**, *36*, 867. [CrossRef]

41. Zhao, Y.; Vaughan, A.S.; Sutton, S.J.; Swingler, S.G. On nucleation and the evolution of morphology in a propylene/ethylene copolymer. *Polymer* **2001**, *42*, 6599. [CrossRef]

42. Foresta, T.; Piccarolo, S.; Goldbeck-Wood, G. Competition between α and γ phases in isotactic polypropylene: Effects of ethylene content and nucleating agents at different cooling rates. *Polymer* **2001**, *42*, 1167. [CrossRef]

43. Marega, C.; Marigo, A.; Saini, R.; Ferrari, P. The influence of thermal treatment and processing on the structure and morphology of poly(propylene-ran-1-butene) copolymers. *Polym. Int.* **2001**, *50*, 442. [CrossRef]

44. Marigo, A.; Causin, V.; Marega, C.; Ferrari, P. Crystallization of the γ form in random propylene-ethylene copolymers. *Polym. Int.* **2004**, *53*, 2001–2008. [CrossRef]

45. Dimenska, A.; Phillips, P.J. High pressure crystallization of random propylene–ethylene copolymers: α–γ Phase diagram. *Polymer* **2006**, *47*, 5445–5456. [CrossRef]

46. Gahleitner, M.; Tranninger, C.; Doshev, P. Polypropylene Copolymers. In *Polypropylene Handbook, Morphology, Blends and Composites*; Karger-Kocsis, J., Bárány, T., Eds.; Springer Nature: Cham, Switzerland, 2019; Chapter 6; p. 295.

47. Galli, P.; Haylock, J.C.; Simonazzi, T. Manufacturing and properties of polypropylene copolymers. In *Polypropylene: Structure, Blends and Composites. Vol. 2 Copolymers and Blends*; Karger-Kocsis, J., Ed.; Chapman & Hall: London, UK, 1995; p. 1.

48. Fischer, D.; Mülhaupt, R. The influence of regio- and stereoirregularities on the crystallization behaviour of isotactic poly(propylene)s prepared with homogeneous group IVa metallocene/methylaluminoxane Ziegler-Natta catalysts. *Macromol. Chem. Phys.* **1994**, *195*, 1433. [CrossRef]

49. Thomann, R.; Wang, C.; Kressler, J.; Mülhaupt, R. On the γ-Phase of Isotactic Poypropylene. *Macromolecules* **1996**, *29*, 8425–8434. [CrossRef]

50. Thomann, R.; Semke, H.; Maier, R.D.; Thomann, Y.; Scherble, J.; Mülhaupt, R.; Kressler, J. Influence of stereoirregularities on the formation of the γ-phase in isotactic polypropylene. *Polymer* **2001**, *42*, 4597–4603. [CrossRef]

51. Alamo, R.G.; Kim, M.H.; Galante, M.J.; Isasi, J.R.; Mandelkern, L. Structural and Kinetic Factors Governing the Formation of the γ Polymorph of Isotactic Polypropylene. *Macromolecules* **1999**, *32*, 4050–4064. [CrossRef]

52. VanderHart, D.L.; Alamo, R.G.; Nyden, M.R.; Kim, M.H.; Mandelkern, L. Observation of Resonances Associated with Stereo and Regio Defects in the Crystalline Regions of Isotactic Polypropylene: Toward a Determination of Morphological Partioning. *Macromolecules* **2000**, *33*, 6078–6093. [CrossRef]

53. Nyden, M.R.; Vanderhart, D.L.; Alamo, R.G. The conformational structures of defect-containing chains in the crystalline regions of isotactic polypropylene. *Comput. Theor. Comput. Sci.* **2001**, *11*, 175–189. [CrossRef]

54. De Rosa, C.; Auriemma, F.; Di Capua, A.; Resconi, L.; Guidotti, S.; Camurati, I.; Nifant'ev, I.E.; Laishevtsev, I.P. Structure-property correlations in polypropylene from metallocene catalysts: Stereodefective, regioregular isotactic polypropylene. *J. Am. Chem. Soc.* **2004**, *126*, 17040–17049. [CrossRef] [PubMed]

55. Arnold, M.; Henschke, O.; Knorr, J. Copolymerization of propene and higher α-olefins with the metallocene catalyst Et[Ind]2HfCl$_2$/methylaluminoxane. *Macromol. Chem. Phys.* **1996**, *197*, 563–573. [CrossRef]

56. Arnold, M.; Bornemann, S.; Köller, F.; Menke, T.J.; Kressler, J. Synthesis and characterization of branched polypropenes obtained by metallocene catalysis. *Macromol. Chem. Phys.* **1998**, *199*, 2647–2653. [CrossRef]

57. Busse, K.; Kressler, J.; Maier, R.D.; Scherble, J. Tailoring of the α-, β-, and γ-Modification in Isotactic Polypropene and Propene/Ethene Random Copolymers. *Macromolecules* **2000**, *33*, 8775–8780. [CrossRef]

58. Wahner, U.M.; Tincul, I.; Joubert, D.J.; Sadiku, E.R.; Forlini, F.; Losio, S.; Tritto, I.; Sacchi, M.C. 13C NMR Study of Copolymers of Propene with Higher 1-Olefins with New Microstructures by *ansa*-Zirconocene Catalysts. *Macromol. Chem. Phys.* **2003**, *204*, 1738. [CrossRef]

59. Costa, G.; Stagnaro, P.; Trefiletti, V.; Sacchi, M.C.; Forlini, F.; Alfonso, G.C.; Tincul, I.; Wahner, U.M. Thermal Behavior and Structural Features of Propene/1-Pentene Copolymers by Metallocene Catalysts. *Macromol. Chem. Phys.* **2004**, *205*, 383–389. [CrossRef]

60. Stagnaro, P.; Costa, G.; Trefiletti, V.; Canetti, M.; Forlini, F.; Alfonso, G.C. Thermal Behavior, Structure and Morphology of Propene/Higher 1-Olefin Copolymers. *Macromol. Chem. Phys.* **2006**, *207*, 2128–2141. [CrossRef]

61. Alamo, R.G.; VanderHart, D.L.; Nyden, M.R.; Mandelkern, L. Morphological Partitioning of Ethylene Defects in Random Propylene−Ethylene Copolymers. *Macromolecules* **2000**, *33*, 6094–6105. [CrossRef]

62. Hosier, I.L.; Alamo, R.G.; Esteso, P.; Isasi, G.R.; Mandelkern, L. Formation of the α and γ Polymorphs in Random Metallocene-Propylene Copolymers. Effect of Concentration and Type of Comonomer. *Macromolecules* **2003**, *36*, 5623–5636. [CrossRef]

63. Hosier, I.L.; Alamo, R.G.; Lin, J.S. Lamellar morphology of random metallocene propylene copolymers studied by atomic force microscopy. *Polymer* **2004**, *45*, 3441–3455. [CrossRef]

64. Alamo, R.G.; Ghosal, A.; Chatterjee, J.; Thompson, K.L. Linear growth rates of random propylene ethylene copolymers. The change over from γ dominated growth to mixed (α+γ) polymorphic growth. *Polymer* **2005**, *46*, 8774–8789. [CrossRef]

65. Fan, Z.; Yasin, T.; Feng, L. Copolymerization of propylene with 1-octene catalyzed by *rac*-Me$_2$Si(2,4,6-Me$_3$-Ind)$_2$ZrCl$_2$/methyl aluminoxane. *J. Polym. Sci. Part A* **2000**, *38*, 4299. [CrossRef]

66. Stagnaro, P.; Boragno, L.; Canetti, M.; Forlini, F.; Azzurri, F.; Alfonso, G.C. Crystallization and morphology of the trigonal form in random propene/1-pentene copolymers. *Polymer* **2009**, *50*, 5242. [CrossRef]

67. Brull, R.; Pasch, H.; Rauberheimer, H.G.; Sanderson, R.D.; Wahner, U.M. Polymerization of higher linear α-olefins with (CH$_3$)$_2$Si(2-methylbenz[e]indenyl)ZzrCl$_2$. *J. Polym. Sci. Part A Polym. Chem.* **2000**, *38*, 2333. [CrossRef]

68. Van Reenen, A.J.; Brull, R.; Wahner, U.M.; Raubenheimer, H.G.; Sanderson, R.D.; Pasch, H. The copolymerization of propylene with higher, linear α-olefins. *J. Polym. Sci. Part A Polym. Chem.* **2000**, *38*, 4110. [CrossRef]

69. Lovisi, H.; Tavares, M.I.B.; da Silva, N.M.; de Menezes, S.M.C.; de Santa Maria, L.C.; Coutinho, F.M.B. Influence of comonomer content and short branch length on the physical properties of metallocene propylene copolymers. *Polymer* **2001**, *42*, 9791–9799. [CrossRef]

70. Shin, Y.-W.; Uozumi, T.; Terano, M.; Nitta, K.-H. Synthesis and characterization of ethylene–propylene random copolymers with isotactic propylene sequence. *Polymer* **2001**, *42*, 9611. [CrossRef]

71. Shin, Y.-W.; Hashiguchi, H.; Terano, M.; Nitta, K. Synthesis and characterization of propylene-α-olefin random copolymers with isotactic propylene sequence. II. Propylene–hexene-1 random copolymers. *J. Appl. Polym. Sci.* **2004**, *92*, 2949.

72. Hosoda, S.; Hori, H.; Yada, K.; Tsuji, M.; Nakahara, S. Degree of comonomer inclusion into lamella crystal for propylene/olefin copolymers. *Polymer* **2002**, *43*, 7451–7460.

73. Fujiyama, M.; Inata, H. Crystallization and melting characteristics of metallocene isotactic polypropylenes. *J. Appl. Polym. Sci.* **2002**, *85*, 1851. [CrossRef]

74. Xu, J.-T.; Xue, L.; Fan, Z.-Q. Nonisothermal crystallization of metallocene propylene–decene-1 copolymers. *J. Appl. Polym. Sci.* **2004**, *93*, 1724. [CrossRef]

75. Poon, B.; Rogunova, M.; Chum, S.P.; Hiltner, A.; Baer, E. Classification of Homogeneous Copolymers of Propylene and 1-Octene Based on Comonomer Content. *J. Polym. Sci. Polym. Phys.* **2004**, *42*, 4357–4370. [CrossRef]

76. Poon, B.; Rogunova, M.; Hiltner, A.; Baer, E.; Chum, S.P.; Galeski, A.; Piorkowska, E. Structure and Properties of Homogeneous Copolymers of Propylene and 1-Hexene. *Macromolecules* **2005**, *38*, 1232–1243. [CrossRef]

77. Palza, H.; López-Majada, J.M.; Quijada, R.; Benavente, R.; Pérez, E.; Cerrada, M.L. Metallocenic Copolymers of Isotactic Propylene and 1-Octadecene: Crystalline Structure and Mechanical Behavior. *Macromol. Chem. Phys.* **2005**, *206*, 1221–1230. [CrossRef]

78. López-Majada, J.M.; Palza, H.; Guevara, J.L.; Quijada, R.; Martinez, M.C.; Benavente, R.; Pereña, J.M.; Pérez, E.; Cerrada, M.L. Metallocene Copolymers of Propene and 1-Hexene: The Influence of the Comonomer Content and Thermal History on the Structure and Mechanical Properties. *J. Polym. Sci. Polym. Phys. Ed.* **2006**, *44*, 1253–1267. [CrossRef]

79. De Rosa, C.; Auriemma, F.; Ruiz de Ballesteros, O.; Resconi, L.; Camurati, I. Crystallization Behavior of Isotactic Propylene-Ethylene and Propylene-Butene Copolymers: Effect of Comonomers *versus* Stereodefects on Crystallization Properties of Isotactic Polypropylene. *Macromolecules* **2007**, *40*, 6600–6616. [CrossRef]

80. Palza, H.; López-Majada, J.M.; Quijada, R.; Pereña, J.M.; Benavente, R.; Pérez, E.; Cerrada, M.L. Comonomer Length Influence on the Structure and Mechanical Response of Metallocenic Polypropylenic Materials. *Macromol. Chem. Phys.* **2008**, *209*, 2259–2267. [CrossRef]

81. Cerrada, M.L.; Polo-Corpa, M.J.; Benavente, R.; Pérez, E.; Velilla, T.; Quijada, R. Formation of the new trigonal polymorph in Ipp–1-hexene copolymers. Competition with the mesomorphic phase. *Macromolecules* **2009**, *42*, 702–708. [CrossRef]

82. Pérez, E.; Gómez-Elvira, J.M.; Benavente, R.; Cerrada, M.L. Tailoring the formation rate of the mesophase in random propylene-co-1-pentene copolymers. *Macromolecules* **2012**, *45*, 6481–6490. [CrossRef]

83. Boragno, L.; Stagnaro, P.; Forlini, F.; Azzurri, F.; Alfonso, G.C. The trigonal form of i-PP in random C3/C5/C6 terpolymers. *Polymer* **2013**, *54*, 1656–1662. [CrossRef]

84. García-Peñas, A.; Gómez-Elvira, J.M.; Pérez, E.; Cerrada, M.L. Isotactic poly(propylene-co-1-pentene-co-1-hexene) terpolymers: Synthesis, molecular characterization, and evidence of the trigonal polymorph. *J. Polym. Sci. A Polym. Chem.* **2013**, *51*, 3251–3259. [CrossRef]

85. García-Peñas, A.; Gómez-Elvira, J.M.; Barranco-García, R.; Pérez, E.; Cerrada, M.L. Trigonal δ form as a tool for tuning mechanical behavior in poly(propylene-co-1-pentene-co-1-heptene) terpolymers. *Polymer* **2016**, *99*, 112–121. [CrossRef]

86. García-Peñas, A.; Gómez-Elvira, J.M.; Lorenzo, V.; Pérez, E.; Cerrada, M.L. Unprecedented dependence of stiffness parameters and crystallinity on comonomer content in rapidly cooled propylene-co-1-pentene copolymers. *Polymer* **2017**, *130*, 17–25. [CrossRef]

87. Auriemma, F.; De Rosa, C.; Di Girolamo, R.; Malafronte, A.; Scoti, M.; Cipullo, R. Yield behavior of random copolymers of isotactic polypropylene. *Polymer* **2017**, *129*, 235–246. [CrossRef]

88. Auriemma, F.; De Rosa, C.; Di Girolamo, R.; Malafronte, A.; Scoti, M.; Cioce, C. A molecular view of properties of random copolymers of isotactic polypropene. *Adv. Polym. Sci.* **2017**, *276*, 45–92.

89. De Rosa, C.; Scoti, M.; Auriemma, F.; Ruiz de Ballesteros, O.; Talarico, G.; Malafronte, A.; Di Girolamo, R. Mechanical Properties and Morphology of Propene−Pentene Isotactic Copolymers. *Macromolecules* **2018**, *51*, 3030–3040. [CrossRef]

90. De Rosa, C.; Scoti, M.; Auriemma, F.; Ruiz de Ballesteros, O.; Talarico, G.; Di Girolamo, R.; Cipullo, R. Relationships among lamellar morphology parameters, structure and thermal behavior of isotactic propene-pentene copolymers: The role of incorporation of comonomeric units in the crystals. *Eur. Polym. J.* **2018**, *103*, 251–259. [CrossRef]

91. De Rosa, C.; Scoti, M.; Ruiz de Ballesteros, O.; Di Girolamo, R.; Auriemma, F.; Malafronte, A. Propylene-Butene Copolymers: Tailoring Mechanical Properties from Isotactic Polypropylene to Polybutene. *Macromolecules* **2020**, *53*, 4407–4421. [CrossRef]

92. Scoti, M.; De Stefano, F.; Di Girolamo, R.; Talarico, G.; Malafronte, A.; De Rosa, C. Crystallization of Propene-Pentene Isotactic Copolymers as an Indicator of the General View of the Crystallization Behavior of Isotactic Polypropylene. *Macromolecules* **2022**, *55*, 241. [CrossRef]

93. Alamo, R.G.; Blanco, J.A.; Agarwal, P.K.; Randall, J.C. Crystallization Rates of Matched Fractions of MgCl2-Supported Ziegler Natta and Metallocene Isotactic Poly(Propylene)s. 1. The Role of Chain Microstructure. *Macromolecules* **2003**, *36*, 1559–1571. [CrossRef]

94. Randall, J.C.; Alamo, R.G.; Agarwal, P.K.; Ruff, C.J. Crystallization Rates of Matched Fractions of MgCl2-Supported Ziegler-Natta and Metallocene Isotactic Poly(propylene)s. 2. Chain Microstructures from a Supercritical Fluid Fractionation of a MgCl2-Supported Ziegler−Natta Isotactic Poly(propylene). *Macromolecules* **2003**, *36*, 1572–1584. [CrossRef]

95. De Rosa, C.; Ruiz de Ballesteros, O.; Auriemma, F.; Talarico, G.; Scoti, M.; Di Girolamo, R.; Malafronte, A.; Piemontesi, F.; Liguori, D.; Camurati, I.; et al. Crystallization Behavior of Copolymers of Isotactic Poly(1-butene) with Ethylene from Ziegler−Natta Catalyst: Evidence of the Blocky Molecular Structure. *Macromolecules* **2019**, *52*, 9114–9127. [CrossRef]

96. De Rosa, C.; Ruiz de Ballesteros, O.; Di Girolamo, R.; Malafronte, A.; Auriemma, F.; Talarico, G.; Scoti, M. The blocky structure of Ziegler–Natta "random" copolymers: Myths and experimental evidence. *Polym. Chem.* **2020**, *11*, 34–38. [CrossRef]

97. Gahleitner, M.; Jääskeläinen, P.; Ratajski, E.; Paulik, C.; Reussner, J.; Wolfschwenger, J.; Neißl, W. Propylene-ethylene random copolymers: Comonomer effects on crystallinity and application properties. *J. Appl. Polym. Sci.* **2005**, *95*, 1073–1081. [CrossRef]

98. Caveda, S.; Pérez, E.; Blázquez-Blázquez, E.; Peña, B.; van Grieken, R.; Suárez, I.; Benavente, R. Influence of structure on the properties of polypropylene copolymers and terpolymers. *Polym. Test.* **2017**, *62*, 23–32. [CrossRef]

99. Auriemma, F.; De Rosa, C.; Di Girolamo, R.; Malafronte, A.; Scoti, M.; Mitchell, G.R.; Esposito, S. Relationship between molecular configuration and stress induced phase transitions. In *Controlling the Morphology of Polymers—Multiple Scales of Structure and Processing*; Mitchell, G.R., Tojeira, A., Eds.; Springer International Publishing: Cham, Switzerland, 2016; p. 287.

100. Auriemma, F.; De Rosa, C.; Di Girolamo, R.; Malafronte, A.; Scoti, M.; Mitchell, G.R.; Esposito, S. Deformation of Stereoirregular Isotactic Polypropylene across Length Scales. Influence of Temperature. *Macromolecules* **2017**, *50*, 2856–2870. [CrossRef]

101. Auriemma, F.; De Rosa, C.; Di Girolamo, R.; Malafronte, A.; Scoti, M.; Mitchell, G.R.; Esposito, S. Time-resolving study of stress-induced transformations of isotactic polypropylene through wide angle X-ray scattering measurements. *Polymers* **2018**, *10*, 162. [CrossRef]

102. De Rosa, C.; Di Girolamo, R.; Auriemma, F.; Talarico, G.; Scarica, C.; Malafronte, A.; Scoti, M. Controlling Size and Orientation of Lamellar Microdomains in Crystalline Block Copolymers. *ACS Appl. Mater. Interfaces* **2017**, *9*, 31252. [CrossRef]

103. Auriemma, F.; De Rosa, C.; Scoti, M.; Di Girolamo, R.; Malafronte, A.; Talarico, G.; Carnahan, E. Unveiling the Molecular Structure of Ethylene/1-Octene Multi-block Copolymers from Chain Shuttling Technology. *Polymer* **2018**, *154*, 298. [CrossRef]

104. Stehling, U.; Diebold, J.; Kirsten, R.; Roell, W.; Brintzinger, H.-H.; Juengling, S.; Mülhaupt, R.; Langhauser, F. ansa-Zirconocene Polymerization Catalysts with Anelated Ring Ligands—Effects on Catalytic Activity and Polymer Chain Length. *Organometallics* **1994**, *13*, 964. [CrossRef]

105. Langhauser, F.; Kerth, J.; Kersting, M.; Koelle, P.; Lilge, D.; Mueller, P. Propylene polymerization with metallocene catalysts in industrial processes. *Angew. Makromol. Chem.* **1994**, *223*, 155. [CrossRef]

106. Resconi, L.; Guidotti, S.; Morhard, F.; Fait, A. Process for the Preparation of 1-butene/propylene Copolymers. U.S. Patent No. 7,531,609, 12 May 2009.

107. Resconi, L.; Guidotti, S.; Camurati, I.; Frabetti, R.; Focante, F.; Nifant'ev, I.E.; Laishevtsev, I.P. C1-Symmetric Heterocyclic Zirconocenes as Catalysts for Propylene Polymerization, 2. *ansa*-Zirconocenes with Linked Dithienocyclopentadienyl-Substituted Indenyl Ligands. *Macromol. Chem. Phys.* **2005**, *206*, 1405. [CrossRef]

108. Resconi, L.; Camurati, I.; Malizia, F. Metallocene Catalysts for 1-Butene Polymerization. *Macromol. Chem. Phys.* **2006**, *207*, 2257. [CrossRef]

109. Covezzi, M.; Fait, A. Process and Apparatus for Making Supported Catalyst Systems for Olefin Polymerization. U.S. Patent No. 7,041,750, 9 May 2006.

110. Randall, J.C. A ^{13}C NMR Determination of the Comonomer Sequence Distributions in Propylene-Butene-1 Copolymers. *Macromolecules* **1978**, *11*, 592. [CrossRef]

111. Kakugo, M.; Naito, Y.; Mizunuma, K.; Miyatake, T. Carbon-13 NMR determination of monomer sequence distribution in ethylene-propylene copolymers prepared with δ-TiCl$_3$-Al(C$_2$H$_5$)$_2$Cl. *Macromolecules* **1982**, *15*, 1150. [CrossRef]